


“Trend analysis and artificial neural networks forecasting for rainfall prediction”

AUTHORS

Oseni Taiwo Amoo
Bloodless Dzwairo  <http://orcid.org/0000-0002-0127-2978>
ResearcherID: [L-3155-2015](https://orcid.org/0000-0002-0127-2978)

ARTICLE INFO

Oseni Taiwo Amoo and Bloodless Dzwairo (2016). Trend analysis and artificial neural networks forecasting for rainfall prediction. *Environmental Economics*, 7(4-1), 149-160. doi:[10.21511/ee.07\(4-1\).2016.07](https://doi.org/10.21511/ee.07(4-1).2016.07)

DOI

[http://dx.doi.org/10.21511/ee.07\(4-1\).2016.07](http://dx.doi.org/10.21511/ee.07(4-1).2016.07)

RELEASED ON

Wednesday, 21 December 2016

JOURNAL

"Environmental Economics"

FOUNDER

LLC "Consulting Publishing Company "Business Perspectives"



NUMBER OF REFERENCES

0



NUMBER OF FIGURES

0



NUMBER OF TABLES

0

© The author(s) 2026. This publication is an open access article.

Oseni Taiwo Amoo (South Africa), Bloodless Dzwairo (South Africa)

Trend analysis and artificial neural networks forecasting for rainfall prediction

Abstract

The growing severe damage and sustained nature of the recent drought in some parts of the globe have resulted in the need to conduct studies relating to rainfall forecasting and effective integrated water resources management. This research examines and analyzes the use and ability of artificial neural networks (ANNs) in forecasting future trends of rainfall indices for Mkomazi Basin, South Africa. The approach used the theory of back propagation neural networks, after which a model was developed to predict the future rainfall occurrence using an environmental fed variable for closing up. Once this was accomplished, the ANNs' accuracy was compared against a traditional forecasting method called multiple linear regression. The probability of an accurate forecast was calculated using conditional probabilities for the two models. Given the accuracy of the forecast, the benefits of the ANNs as a vital tool for decision makers in mitigating drought related concerns was enunciated.

Keywords: artificial neural networks, drought, rainfall case forecast, multiple linear regression.

JEL Classification: C53, C45.

Introduction

Rainfall is a natural climatic feature whose forecasting is challenging and demanding, as the world continues to observe ever varying climate circumstances. Its prediction plays a significant role in water resources management and, therefore, it is of particular relevance to the agricultural sector, which adds majorly to the economy of any country (Abdulkadir, Salami and Kareem, 2012). Rainfall occurrence is one of the most complex elements of the hydrological cycle whose understanding has been subjected to a large range of change over space and time (French, Krajewski and Cuykendall, 1992). Furthermore, the interwoven nature of the atmospheric processes that generate rainfall makes reckonable prediction of rainfall an exceedingly difficult chore (Hung et al., 2009).

In recent years, the parameterization and uncertainties associated with process-based models have shifted the drift to the use of data-driven modeling techniques. Thus, smart technology has helped with information abstraction from data in detecting and predicting the likelihood of event trending. Data-driven models are usually numerical based information that employ statistical and mathematical concepts to link a certain input (rainfall) to the model output (runoff). However, the various techniques often use system identification, regression, transfer functions, and neural networks (Solomatine and Ostfeld, 2008). On the other hand, traditional time series (moving average) trending and multiple linear regression analysis have been

used to test the variability, homogeneity and trending patterns of rainfall series over a time period.

Hence, the challenge posed by the non-linear nature of rainfall has been argued against the traditional methods which use independent variables that are highly correlated with each other. These cannot determine, which independent variables best predict the dependent variable without duplicating characteristics (Paswan and Begum, 2013). Thus, the advent of digital computer neural simulation has made data driven techniques substitute forecasting tools in time series, which is useful for rainfall prediction. The neural network regression (NNR) is most suited to problems, where a more traditional regression model cannot fit a solution. The NNR model uses adaptive weight functions when approximating non-linear functions of their inputs.

This study presented herein, the suitability of Multilayer Perceptron (MLP) neuron as a back propagating neuron in transferring functions to a hidden layer for predicting rainfall cases.

Another tool called Back Propagation algorithm Network (BPN) (Rumelhart et al., 1986) emulates the human nerve system by the gradient descent method. It has certain performance characteristics resembling biological neural networks of the human brain (Haykin, 1994). This has proven to be helpful in dealing with complicated problems such as function approximation, pattern recognition and time series prediction. The BPN algorithm can be summarized as operating by way of a forward pass and a backward pass. All of the weights are fixed in the forward pass, but they are adjustable in the backward pass. Furthermore, training a neural network in the backward pass achieves optimization most effectively by adjusting the weights and thresholds.

© Oseni Taiwo Amoo, Bloodless Dzwairo, 2016.

Oseni Taiwo Amoo, Department of Civil Engineering and Surveying, Durban University of Technology, South Africa.

Bloodless Dzwairo, Dr., Department of Civil Engineering: Pietermaritzburg, Durban University of Technology, South Africa.

ANNs have been reported (Barua et al., 2010; Dorofki et al., 2012; Paswan and Begum, 2013) to provide best performance among the data-driven models despite considerable influence by the problems of overfitting and memorization when subjected to small amounts of datasets. The limited number of data length not only affects its performance, but also questions whether the most significant patterns are included or not (Gosasang, Chandraprakaikul and Kiattisin, 2011). This study tested multiple combinations of the hidden functions in finding optimal configuration settings for predicting the rainfall case. The paper compared the ANNs model with a traditional multiple linear regression model for predicting rainfall occurrence using three environmental-fed variables; temperature, wind speed and humidity. The accuracy of the forecast was calculated using a conditional probabilities goodness of fit test.

An ANNs is a vast parallel-distributed information processing system that has become a refined tool, which is used in various hydrology related areas since the early nineties. It has been used in deep-learning and for modeling complex problems such as rainfall-runoff modeling (French, Krajewski and Cuykendall, 1992; Valluru and Rao, 2011), stream flow forecasting (Chang and Chen, 1998), ground-water modeling (Chang and Chen, 2001), water quality (Chang and Chen, 2003), water management policy and precipitation forecasting (Hjelmfelt and Wang, 1993; Ekhmaj, 2010) and hydrologic time series and reservoir operations. Dzwauro (2011) described ANNs as one of the two approaches

(the other being genetic algorithms) which appear to be most innovative for ecological modelling. All the given scenarios can, thus, be easily adapted to regression problems. Other network topologies that have found application in hydrology include radial backward feeding (Chang and Chen, 2003; Barua et al., 2010; Luce, 2014).

Numerous learning algorithms have been used for the purpose of training and subjecting ANNs to adaptive learning. The popular one includes methods based on gradient descent such as back propagation (BP) algorithm, quick propagation (QP) algorithm, Levenberg Marquardt (LM) algorithm, the evolutionary-heuristic methods such as genetic algorithm (GA), and differential evolution (DE) algorithm (Oyebode, Adeyemo and Otieno, 2014). The results from all these models performance were of good output value.

Multilayer Perceptron (MLP) has been a unique and commonly used class of ANNs for back propagation algorithm. It operates on supervised training in that the derived response of the network (target value) for each input pattern is always available. The algorithm uses an activation function (transfer function) to limit the amplitude of the output of a neuron to some finite value. Its structure incorporates individual inputs X_1, X_2, \dots, X_n multiplied by the corresponding elements $W_{i1}, W_{i2}, \dots, W_{in}$ of the weight matrix W . The schematic diagram of the MLP configuration is shown in Fig. 1.

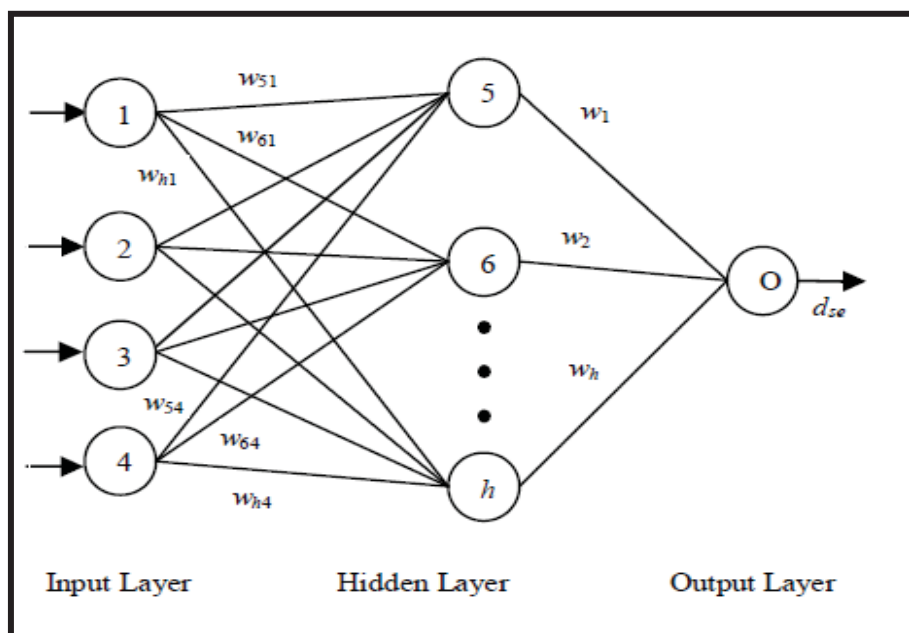


Fig. 1. A simple 3-layer feedforward neural network

The configuration unit description is as follows: $w_{i,j}$ is the weight between j^{th} input node and i^{th} hidden node;

$w_{i,k}$'s are the weights between hidden and output nodes.

The knowledge learnt by the network is stored in the arcs and nodes in the form of arc weights and node biases, which is the key element of ANNs. It is through the linking arcs that ANNs can carry out complex nonlinear mapping from its input nodes to its output nodes. The inherent ability to adjust weights and adapt nature to a system seems suitable to use ANNs in handling nonlinear systems such as rainfall forecasting (Sudheer, Gosain and Ramasastri, 2002).

Due to the differentiable property of log-sigmoid transfer function, it is the most commonly used in multilayer perceptron trained backpropagation algorithm (ASCE, 2000). The hyperbolic tangent sigmoid (Tan-sigmoid) activation function is also used in training the hidden layers to take input in the range of plus infinity to minus infinity, but squashes the output into the range -1 to +1. These are as shown in equations 1.1 and 1.2.

- ◆ The sigmoid (logistic) function

$$f(x) = (1 + \exp(-x))^{-1} \tag{1.1}$$

- ◆ The hyperbolic tangent (tan h) function

$$f(x) = (\exp(x) - \exp(-x)) / (\exp(x) + \exp(-x)) \tag{1.2}$$

For a casual forecasting problem, the inputs to ANNs are usually the independent or predictor variables. The functional relationship estimated by the ANNs can be written as in equation 1.3:

$$Y = f(X_1, X_2, \dots, X_n), \tag{1.3}$$

where X_1, X_2, \dots, X_n are the independent variables and Y is an dependent variable. In this sense, the neural network is functionally equivalent to a nonlinear regression model.

On the other hand, for an extrapolative or time series forecasting problem, the inputs are typically the past observation of the data series and the output is the future value (Sudheer, Gosain and Ramasastri, 2002; Aqil et al., 2007). The ANNs perform the following mapping as in equation 1.4.

$$Y_{t+1} = f(Y_t, Y_{t+1}, \dots, Y_{t-n}), \tag{1.4}$$

where Y_t is the observation at time (t). Thus, the ANNs are equivalent to the nonlinear autoregressive model for time series forecasting problems (Wilby et al., 1998).

Linear regression (as shown in equation 1.5) assumes that the expected value of the output given an input $E[Y / X]$ is linear.

That is,

$$Out(x) = wx. \tag{1.5}$$

The original series can be plotted together with the moving average series to depict the trend (equation 1.6). Therefore,

$$Y_i = wx_i + noise, \tag{1.6}$$

where the noise signals are independent (Hung et al., 2009). The function $P(Y/w, x)$ has a normal distribution with mean (wx) and variance (δ^2) , giving a maximum likelihood w , which minimizes the sum of squares of residuals in equation 1.7. Therefore, equation 1.5 is the same as equation 1.7, which can be used for prediction.

$$E = \sum_i (Y_i - wx_i)^2. \tag{1.7}$$

Neural Network Regression uses the trend approach acquired during the neural training. The signal output y can be expressed in a mathematic form as in equation 1.8:

$$Y_j = f(X \cdot W_j - b_j) \tag{1.8}$$

The sum of the product of the inputs and their relative weights decides the sensitivity of the ANNs. If the summation is greater than the threshold value, an output is computed using a function f . This can be further broken down to equation 1.9:

$$Y = S_1 \left(\sum_{j=1}^{ij} O_j \cdot w_j + w_{ij} \right), \tag{1.9}$$

where Y is the output and O_j is the output value of the j^{th} hidden node (equation 1.10):

$$O_j = S_2 \left(\sum_{x=1}^n X_x \cdot w_{ij} + w_{oj} \right), \tag{1.10}$$

w_i are the connection weights between nodes of the hidden and output layer,

w_{ij} are the connection weights between nodes of the hidden and the input layer,

$X_o = 1.0$ is a bias and w_o and w_{oj} are the weights for the biases,

S_1 and S_2 are activation functions.

For optimum performance, training data was transformed into the log function using equation 1.11:

$$z = 0.5 * \log_{10}(x + 1), \tag{1.11}$$

where x is the input.

Bias and relative bias are measures of systematic errors in the forecast; the biases prevent surface error from continuously passing through the origin at all times. Therefore, measure the degree to which the forecast is consistently above or below the actual value over a period of many years (Gosasang, Chandraprakaikul and Kiattisin, 2011).

Equations 1.12 to 1.18 have been widely used measures of forecast errors (Wonham, 1974; Adegboye and Ipinyomi, 1995; Antonopoulos, Papamichail and Mitsiou, 2001; Ogaji and Singh, 2006; Barua et al., 2010):

i Bias: $B = M_F - M_o$ (1.12)

ii Relative Bias = $RB = \frac{B}{M_o}$ (1.13)

iii Mean Absolute error:

$$MAE = n^{-1} \sum_{i=1}^n |Q_{obs}(i) - Q_{pred}(i)| \tag{1.14}$$

iv Coefficient of correlation:

$$(r) = \pm \sqrt{\frac{\sum(Q_{est} - Q_{mean})^2}{\sum(Q_{obs} - Q_{mean})^2}} \tag{1.15}$$

v Root mean squared error: $RMSE = (MSE)^{0.5} = \sqrt{n^{-1} \sum_{i=1}^n \{Q_{obs}(i) - Q_{pred}(i)\}^2}$ (1.16)

vi Relative mean absolute error:

$$RMAE (RB) = \frac{MAE}{M_o} \tag{1.17}$$

vii R squared: $R^2 = \frac{E_o - E}{E_o}$, (1.18)

where $E = \sum_i^N (Q_{i(obs)} - Q_{i(est)})^2$

The normalized Root Mean Square Error (equation 1.16), which is the sum of squared errors (SSE) normalized the number of testing patterns over all the output nodes was chosen as the performance indicator. This resulted in absolute error measures, which were less dominated by a small number of large errors, and were, thus, a more reliable indicator of typical error magnitude. The above approach was used in the current study and specifically for this paper.

1. Materials and methods

1.1. Study area and datasets. The Mkomazi River is located within the semi-arid province of KwaZulu-Natal in South Africa. It lies in South Africa’s primary basin called Mvoti/uMgeni/Mkomazi or U (see Fig. 2). It is the third longest in the province (Oyebode, Adeyemo and Otieno, 2014). The river has several large tributaries which include Lotheni, Nzinga, Mkomanzana and Elands rivers (Fig. 3).

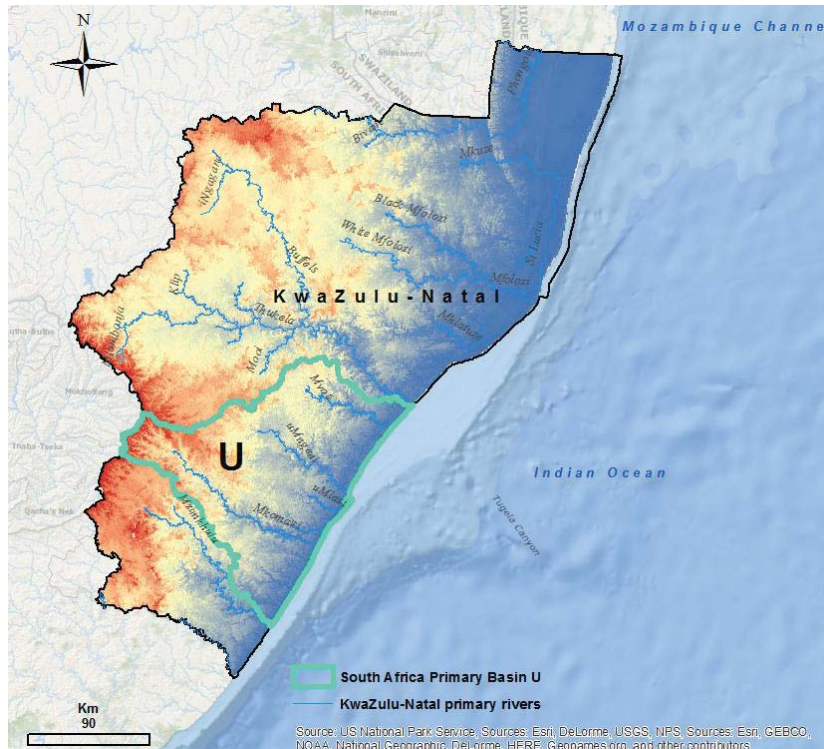


Fig. 2. Mvoti/uMgeni/Mkomazi primary basin (U) in KwaZulu-Natal province

Data source: ESRI online data and Department of Water and Sanitation GIS shape files.

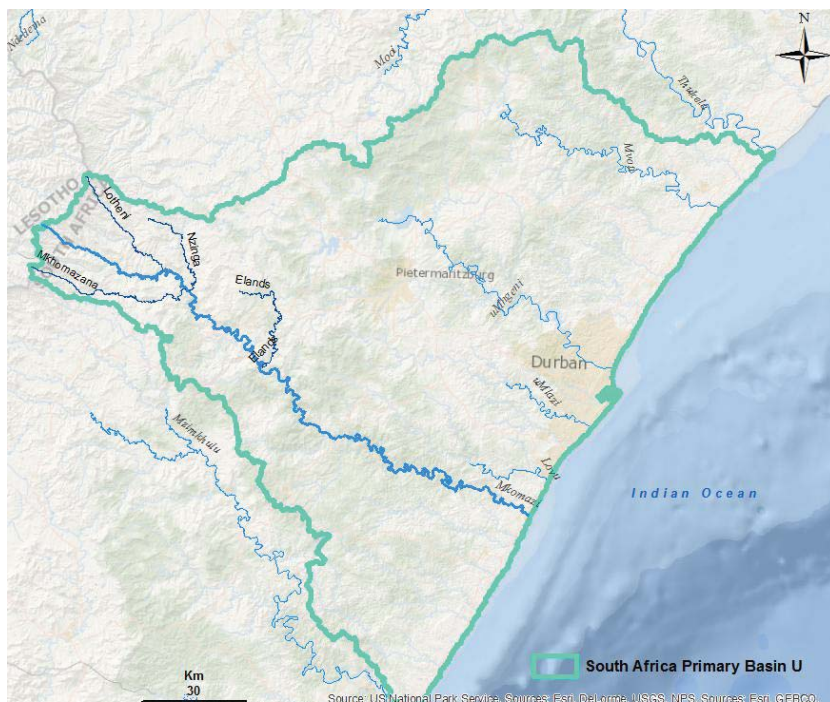


Fig. 3. Mkomazi River inside the primary basin U.

Data source: ESRI online data, Department of Water and Sanitation and internet GIS shape files

Neural Networks Regression was used for rainfall prediction in this study at the upper part of Mkomazi River. Historical records of environmental and meteorological variables for a 16-year period (1990-2015) were used for model predictor variables development, which served as the input vector space.

Datasets relating to the study area were provided by the South African Weather Services (SAWS).

These include historical mean monthly records of climatic data (rainfall, temperature, humidity and wind speed) for stations namely Shaleburn and Giant Castle (IFS site 1). These are located within the study area, while U1H005 (Mkomazi River @ Lot 93 1821) is on geographical coordinates $Y = -29,744$ and $X = 29,906$ (Fig. 4).

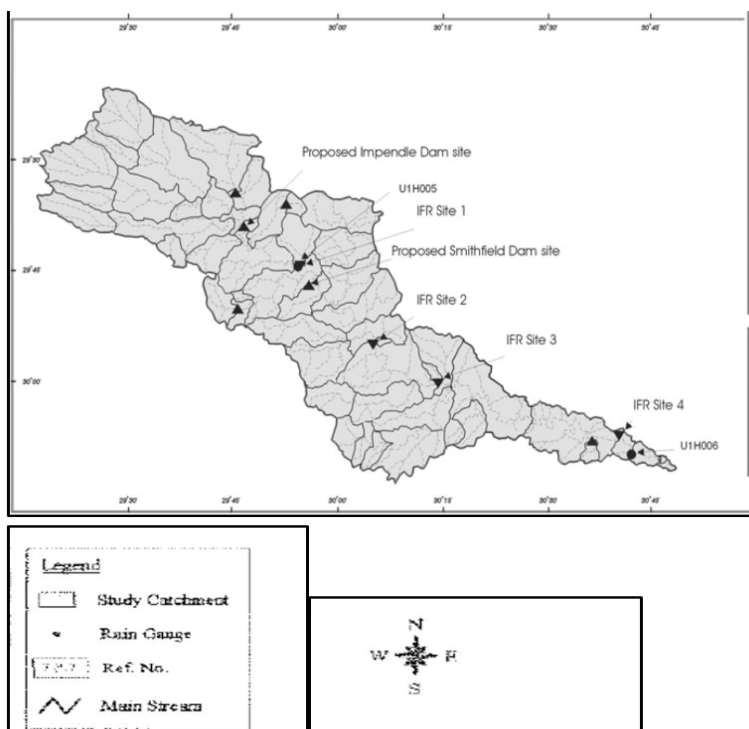


Fig. 4. The study location

Location of only Mkomazi River gauging stations is provided in Fig 5, for clarity.

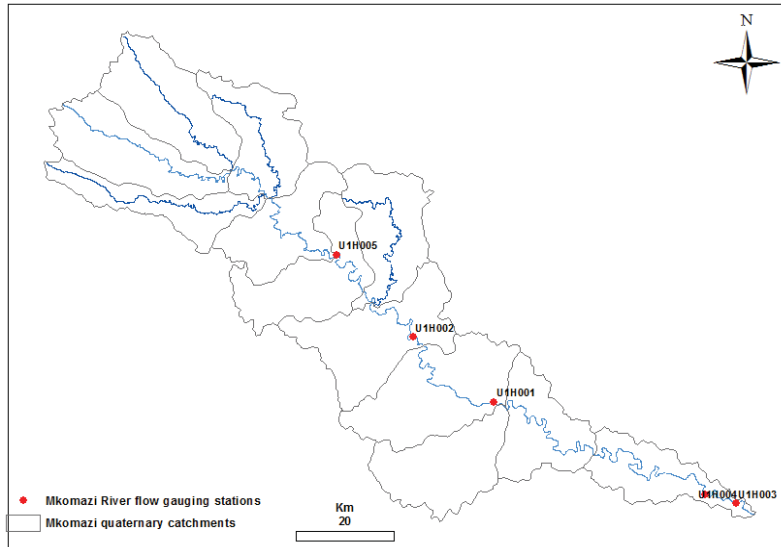


Fig. 5. Location of only Mkomazi River gauging stations (as at 11 November 2016)

1.2. ANNs methods and analysis. The MLP neural network model was implemented in a Matlab 2015a environment. The dataset

consisted of four elements for climatic data and 311 instances for the combined stations. Fig. 6 shows the software interface.

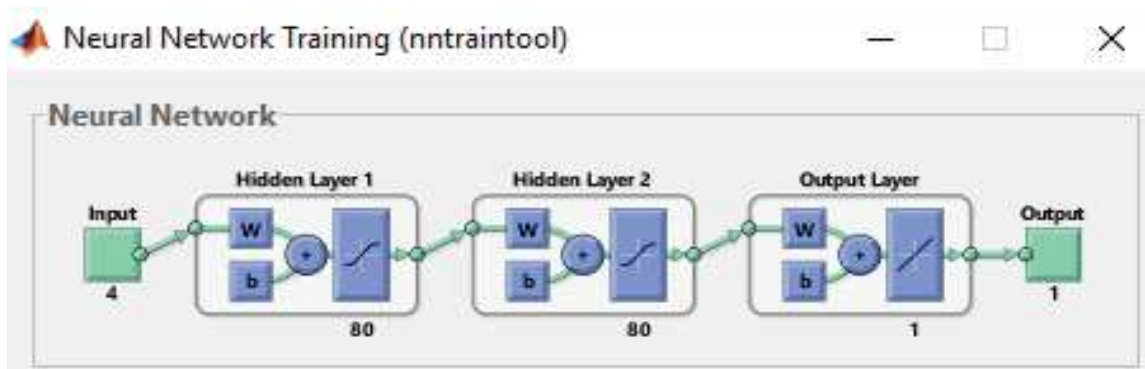


Fig. 6. Neural network training in a Matlab environment

The above ANNs configuration was made after several trials transfer function in the hidden layers for the training and testing section. Optimal weights of ANNs that gave the closest output value consist of two hidden layers, with eighty neurons for each layer at maximum 500 iterations. The tansig and tainseg transfer function in the hidden layer gave the best performance at executive time 0.09 second. These transfer functions were tested after training by the algorithm of Back Propagation Network (BPN) to build a best fit model for a rainfall case forecast.

To train the network, the datasets were divided randomly into a training set and a testing set. The training and testing set consisted of 70% and 30% data points, respectively. For effective training of the network, the dataset was normalized using equation 1.11. The combined environmental variables of the two stations for the catchment were taken as

the input data, while the rainfall data were the output data to be forecasted.

1.3. Multiple linear regression method of analysis. In determining the multiple linear regression between mean monthly rainfall and meteorological collected environmental variables, the ‘Linest’ function in Excel was used to match known data points towards solving the regression analysis. The regression equation for mean monthly rainfall prediction follows the model (equation 1.19).

$$P = -5.5a_1 + 9.2a_2 - 33.2a_3 + 1.3a_4 + 110, \quad (1.19)$$

where P is the station mean monthly rainfall (mm),

while a_1 , a_2 , a_3 , a_4 are the maximum temperature (°C), minimum temperature (°C), wind speed (m/s), and humidity (%), respectively. Table 1 presents the summary of the regression output, while Fig. 7 shows the correlated best line plot.

Table 1. Summary of the regression analysis

| Regression statistics | | | | | | |
|-----------------------|-----------|--|-----------|-----------|-------------|-----------------------|
| Multiple R | 0.768366 | | | | | |
| R Square | 0.590386 | | | | | |
| Adjusted R Square | 0.585032 | | | | | |
| Standard error | 45.11894 | | | | | |
| Observations | 311 | | | | | |
| | <i>df</i> | | <i>SS</i> | <i>MS</i> | <i>F</i> | <i>Significance F</i> |
| Regression | 4 | | 897843.3 | 224460.8 | 110.2612028 | 4.50764E-58 |
| Residual | 306 | | 622930 | 2035.719 | | |
| Total | 310 | | 1520773 | | | |

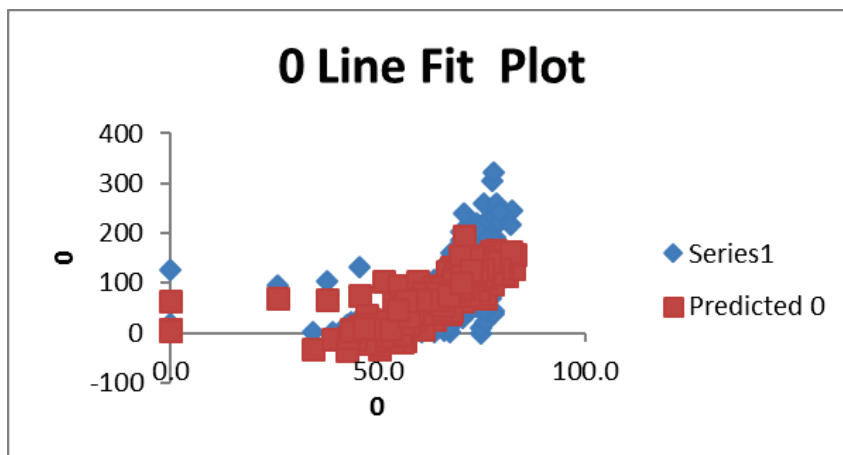


Fig. 7. The correlated best line plot

2. Results and discussion

Comparison of rainfall trending at the study area shows that extreme rainfall events (droughts) occurred during the last decades. Fig. 8 and 9 show the decreasing inter annual trend of rainfall for the two

stations data recorded by SAWS Bureau. The mean annual rainfall was less than 500 mm far less than required mean average 865 mm (Taylor, Schulze and Jewitt, 2003). This shows that there has been increasing trend of dryer climatic conditions at both stations, respectively.

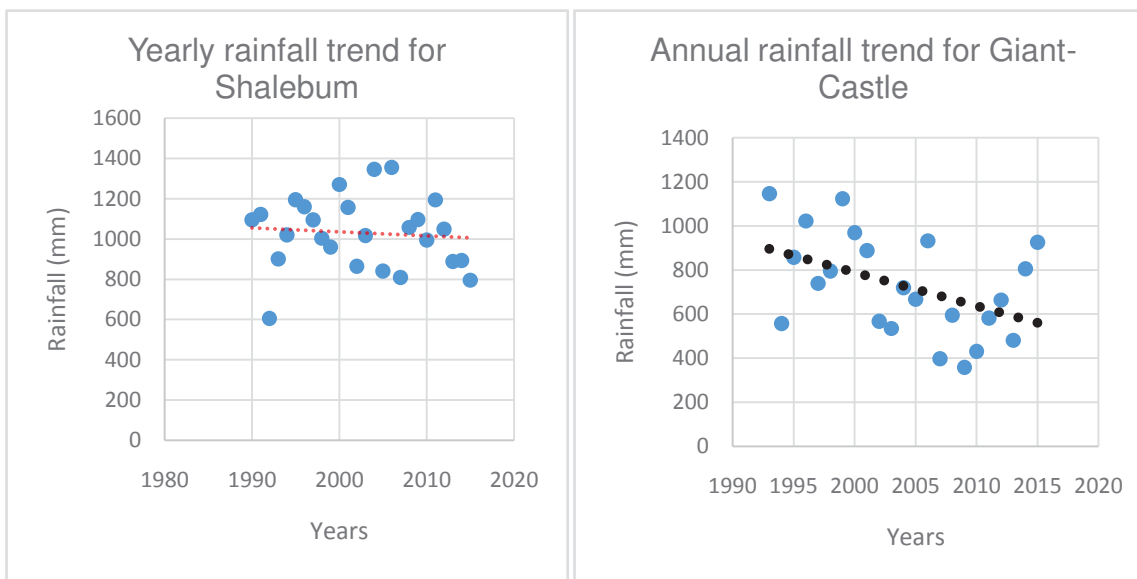


Fig. 8. The sharp decline in annual rainfall for Mkomazi catchment

This was more pronounced for the months between May to July, as depicted in Fig. 8 during the years

(1990-2015) under consideration. Fig. 9 showed the plotted monthly rainfall data analysis trend.

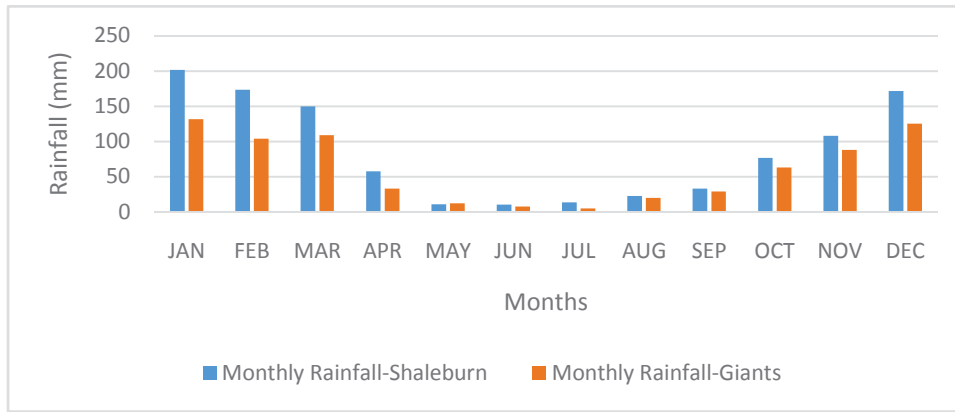


Fig. 9. Plotted monthly rainfall data analysis trend

Fig. 8 and 9 depict the plotted mean annual and monthly rainfall data used for this investigation. There were decreasing trend which reach climax in July before gradual increase in the amount of rainfall. Furthermore, the effects of other monthly meteorological data followed the same rainfall

monthly trend. Fig. 10 and Fig. 11 show the plotted of the monthly averages of humidity and temperature for the period under study. It can be observed from both stations that all follow the same monthly pattern. These was a result of their strong influence towards rainfall occurrence.

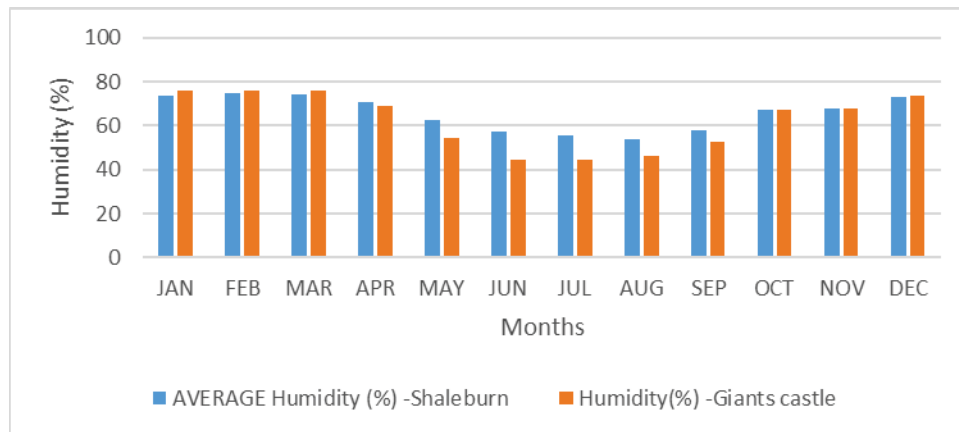


Fig. 10. Plot of average monthly humidity at the two weather stations

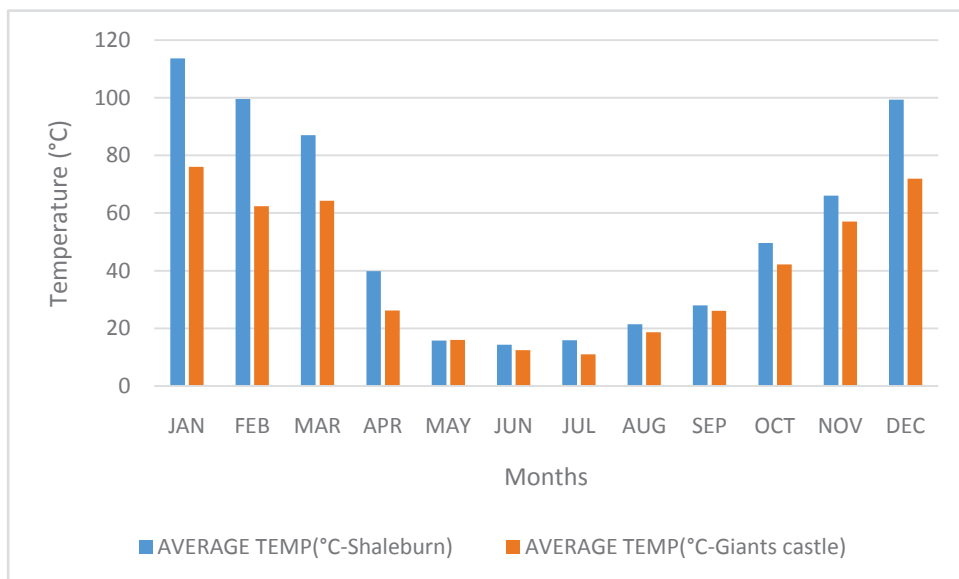


Fig. 11. Plot of average monthly temperature at the two weather stations

An increase in temperature occurs between the months of October and February, after which it follows a downward trend until it reaches its minimum

between the months of June and July. The same was observed for humidity and rainfall. Fig. 12 is the plot for average monthly wind speed.

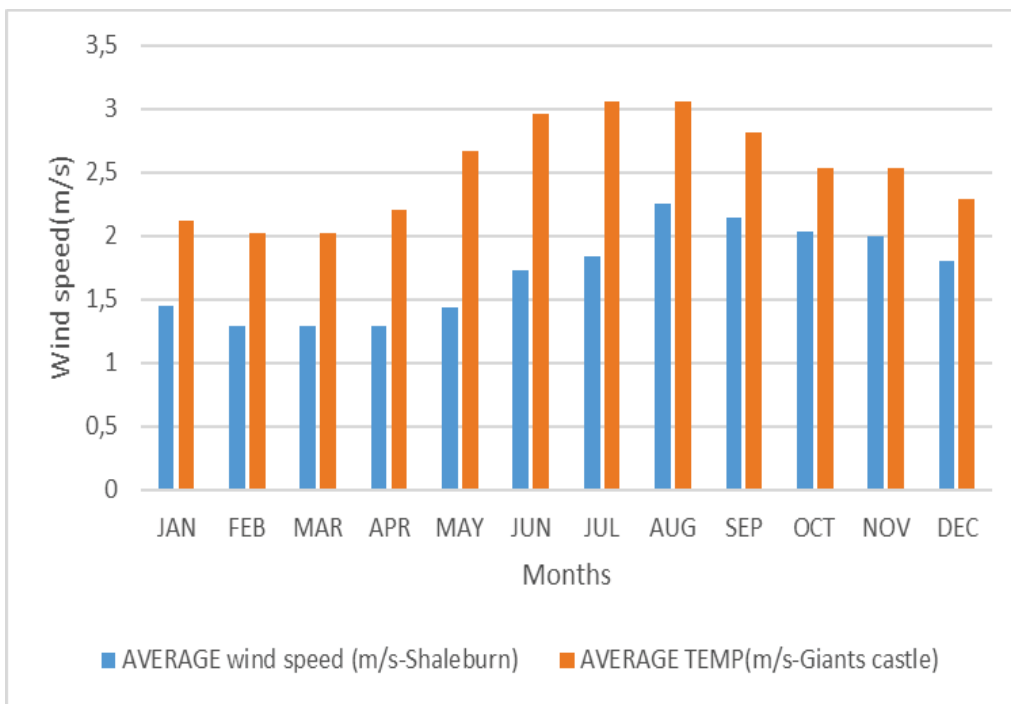


Fig. 12. Plot of average monthly wind speed at the two weather stations

It can be inferred from Fig. 12 that wind speed and rainfall graphs are both mutually exclusive. An upwards trend in one resulted in downward trend for the other. The magnitude of temperature inversely resulted in low humidity and wind speed, which adversely affected the magnitude of rainfall over the catchment area.

2.1. Model performance and evaluation.
The performance of the ANNs configuration and

MLR was evaluated using the statistical functions root mean square error (RMSE) and correlation coefficient (CC), based on the training and testing results. The model which resulted in minimum RMSE and maximum CC value was considered as the best. An optimum model gave closest y- estimated value to the observed value. Table 2 is the tabulated sample of results for the two models.

Table 2. Estimated comparison of both models which predicted rainfall case value

| | Y observed sample (mm) | ANNs estimated | MLR predicted |
|----------|------------------------|----------------|---------------|
| | 175.9 | 178.1 | 144.1 |
| | 20.9 | 24.8 | 44.23 |
| | 37.7 | 47.1 | 13.1 |
| | 106.3 | 129.9 | 76.64 |
| | 19.2 | 10.5 | 14.1 |
| | 155.9 | 122.0 | 140.81 |
| Testing | RMSE | 0.034 | 44.9 |
| | CC | 0.84 | 0.76 |
| R Square | | 0.85 | 0.59 |

The training and testing results of the optimum MLP model for the study area rainfall forecasting are plotted in Fig. 1.13. The values of R measure the correlation between the forecasted and actual rainfall values are shown below. It is seen from Fig. 13 that the test

case results for target and predicted values are within ±10% error for the training and validation in ANN, while MLR is in the range of 25% to observed condition probability. ANN model has the minimum RMSE (0.034) and maximum CC (0.84) during testing is selected as optimum.

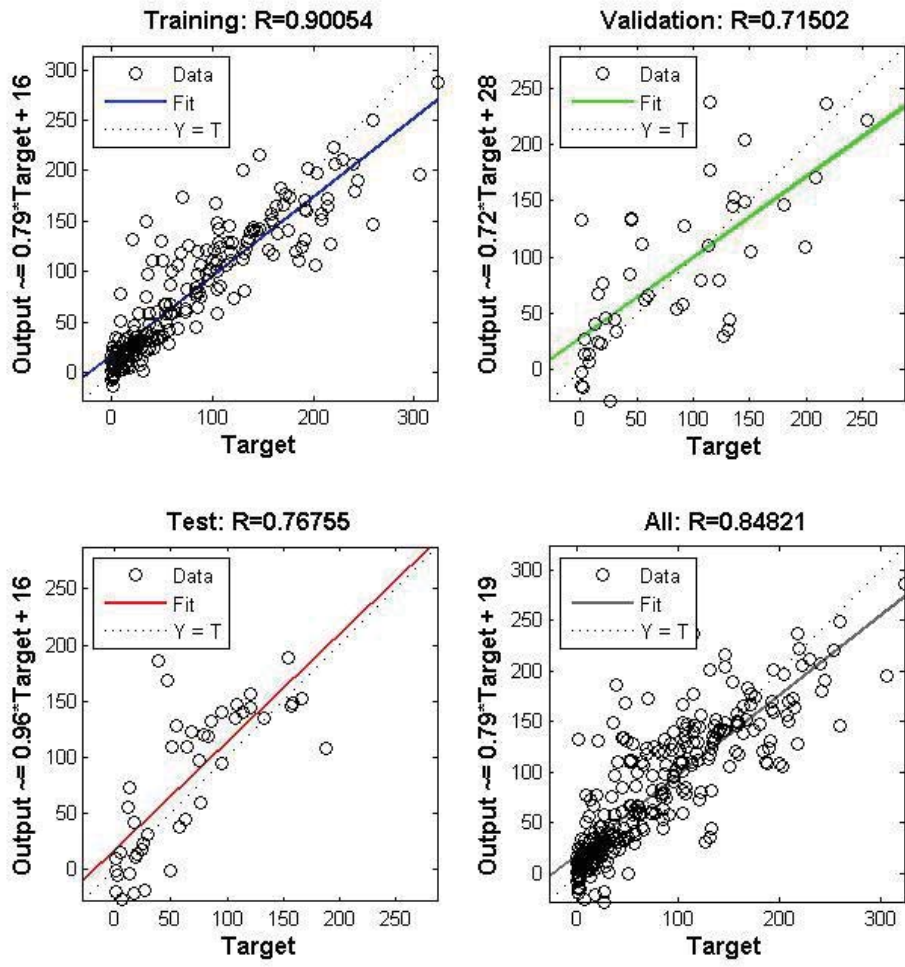


Fig. 13. The training and validation correlation regression for the ANN

Fig. 14 depicts the best performance relationship in the ANNs test.

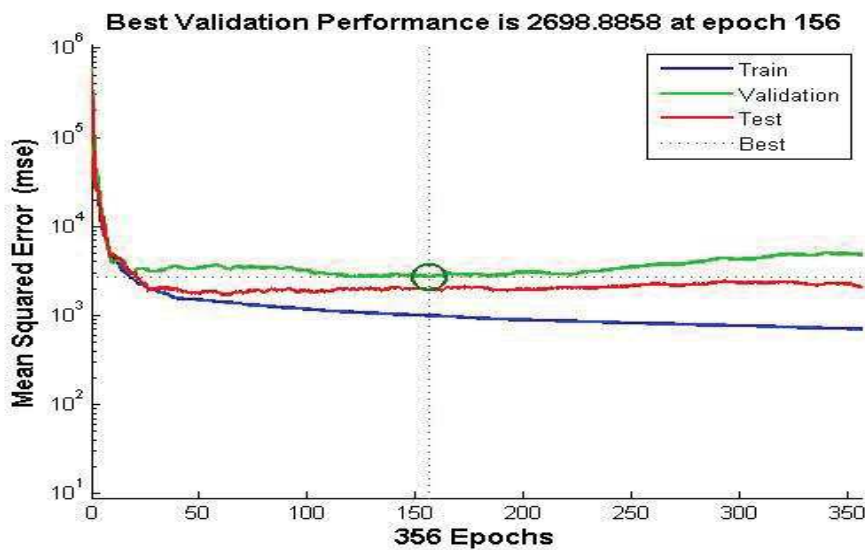


Fig. 14. Shows validation best performance relationship in the ANNs test

The suitability of using neural regression analysis in mitigating against drought and as an adequate tool when it concerns planning and management

of water resources systems in water stressed regions can be effectively employed using above methods. This condition applies if MLR capability is

compared with a complex predictor variable, decision maker with the tools as an effective and efficient mean in quantifying rainfall.

Conclusions

The use of numerical modelling methods, including Dynamic Regression, Conditional Probability Time Series and Artificial Neural Networks has been investigated in this study for the purpose of developing a rainfall case forecast model that is fed by environmental variables.

The ANNs modelling of environmental variables in the upper Mkomazi basin, using MATLAB toolbox, showed that ANNs is a better forecasting tool, since values of R are > 0.5 . Although the results of the trained network were reliable and fitted well during the training of the model, subsequent quantitative prediction of rainfall during validation showed a decline of optimization, since errors observed in

the validation and testing model output were at minimal variance. Most model prediction inherits much error and uncertainty by the underlying empirical risk minimization (ERM) during testing. The values of RMSE suggest that correlation between the forecasted and actual rainfall values in the location were close.

Acknowledgments

The authors would like to acknowledge the support from the South Africa Weather Bureaus for providing the data that were employed in this study. Durban University of Technology is acknowledged for providing the study environment and the South Africa National Research Foundation (NRF) for the finance. The authors are grateful to the anonymous reviewer and editor for their invaluable guidance and constructive comments, which considerably improved the presentation of the paper.

References

1. Abdulkadir, T., Salami, A. and Kareem, A. (2012). Artificial Neural Network of Rainfall in Ilorin, Kwara State, Nigeria, *USEP Research information in Civil Engineering*, 9, pp. 108-120.
2. Adegboye, O. and Ipinoyomi, R. (1995). *Statistical tables for class work and examination*. Ilorin, Nigeria: Tertiary publications Nigeria Limited.
3. Antonopoulos, V.Z., Papamichail, D.M. and Mitsiou, K.A. (2001). Statistical and trend analysis of water quality and quantity data for the Strymon River in Greece, *Hydrology and Earth System Sciences Discussions*, 5(4), pp. 679-692.
4. Aqil, M., Kita, I., Yano, A. and Nishiyama, S. (2007). Analysis and prediction of flow from local source in a river basin using a Neuro-fuzzy modeling tool, *Journal of environmental management*, 85(1), pp. 215-223.
5. ASCE. (2000). Artificial neural networks in hydrology II: Hydrology Applications, *Journal of Hydrologic Engineering*, 5(2), pp. 124-137.
6. Barua, S., Perera, B., Ng, A. and Tran, D. (2010). Drought forecasting using an aggregated drought index and artificial neural network, *Journal of water and climate change*, 1(3), pp. 193-206.
7. Chang, F.-J. and Chen, L. (1998). Real-coded genetic algorithm for rule-based flood control reservoir management, *Water Resources Management*, 12(3), pp. 185-198.
8. Chang, F.-J. and Chen, Y.-C. (2001). A counterpropagation fuzzy-neural network modeling approach to real time streamflow prediction, *Journal of Hydrology*, 245(1), pp. 153-164.
9. Chang, F.-J. and Chen, Y.-C. (2003). Estuary water-stage forecasting by using radial basis function neural network, *Journal of Hydrology*, 270(1), pp. 158-166.
10. Dorofki, M., Elshafie, A.H., Jaafar, O., Karim, O.A. and Mastura, S. (2012). Comparison of artificial neural network transfer functions abilities to simulate extreme runoff data, *International Proceedings of Chemical, Biological and Environmental Engineering*, 33, pp. 39-44.
11. Dzwauro, B. (2011). Modelling raw water quality variability in order to predict cost of water treatment (DTech thesis). D Tech. Eng: Civil Tshwane University of Technology.
12. Ekhmaj, A.I. (2010). Predicting soil infiltration rate using Artificial Neural Network. In Proceedings of 2010 *International Conference on Environmental Engineering and Applications*, IEEE, pp. 117-121.
13. French, M.N., Krajewski, W.F. and Cuykendall, R.R. (1992). Rainfall forecasting in space and time using a neural network, *Journal of Hydrology*, 137(1-4), pp. 1-31.
14. Gosasang, V., Chandraprakaikul, W. and Kiattisin, S. (2011). A comparison of traditional and neural networks forecasting techniques for container throughput at Bangkok port, *The Asian Journal of Shipping and Logistics*, 27(3), pp. 463-482.
15. Haykin, S.S. (1994). *Blind deconvolution*, Prentice Hall.
16. Hjelmfelt, A. and Wang, M. (1993). Runoff simulation using artificial neural networks. In Proceedings of *Proceedings of the Congress-International Association For Hydraulic Research*, Local Organizing Committee of the XXV Congress, pp. 517-517.
17. Hung, N.Q., Babel, M.S., Weesakul, S. and Tripathi, N. (2009). An artificial neural network model for rainfall forecasting in Bangkok, Thailand, *Hydrology and Earth System Sciences*, 13(8), pp. 1413-1425.

18. Luce, C. (2014). *Runoff Prediction in Ungauged Basins: Synthesis Across Processes, Places and Scales*. Wiley Online Library.
19. Ogaji, S. and Singh, R. (2006). Artificial neural networks in fault diagnosis: a gas turbine scenario, *Computational Intelligence in Fault Diagnosis*, Springer, pp. 179-207.
20. Oyebo, O., Adeyemo, J. and Otieno, F. (2014). Monthly stream flow prediction with limited hydro-climatic variables in the upper Mkomazi river, South Africa using genetic programming, *Fresenius Environmental Bulletin*, 23(3), pp. 708-719.
21. Paswan, R.P. and Begum, S.A. (2013). Regression and Neural Networks Models for Prediction of Crop Production 1.
22. Rumelhart, D.E., Hintont, G.E. and Williams, R.J. (1986). *Learning representations by back-propagating errors*.
23. Solomatine, D.P. and Ostfeld, A. (2008). Data-driven modelling: some past experiences and new approaches, *Journal of hydroinformatics*, 10(1), pp. 3-22.
24. Sudheer, K., Gosain, A. and Ramasastri, K. (2002). A data-driven algorithm for constructing artificial neural network rainfall-runoff models, *Hydrological Processes*, 16(6), pp. 1325-1330.
25. Taylor, V., Schulze, R. and Jewitt, G. (2003). Application of the indicators of hydrological alteration method to the Mkomazi River, KwaZulu-Natal, South Africa, *African Journal of Aquatic Science*, 28(1), pp. 1-11.
26. Valluru, S.K. and Rao, T.N. (2011). *Introduction to Neural Networks, Fuzzy Logic and Genetic Algorithms*, Jaico Publishing House, Mumbai.
27. Wilby, R.L., Wigley, T.M.L., Conway, D., Jones, P.D., Hewitson, B.C., Main, J. and Wilks, D.S. (1998). Statistical downscaling of general circulation model output: a comparison of methods, *Water Resources Research*, 34(11), pp. 2995-3008.
28. Wonham, W.M. (1974). Linear multivariable control, *Optimal Control Theory and its Applications*, Springer, pp. 392-424.